

Reactions of diethylgermane, triethylgermane, and ethyl groups on Ge(100)

Jihong Chen^{a)} and C. Michael Greenlief^{b)}

Department of Chemistry, University of Missouri-Columbia, Columbia, Missouri 65211

(Received 1 October 1996; accepted 11 March 1997)

The adsorption and decomposition of diethylgermane and triethylgermane on the Ge(100) surface are investigated. These molecules are potential Ge sources for the deposition of epitaxial Ge thin films. Room temperature adsorption of either ethylgermane leads to the formation of surface germanium hydrides and ethyl groups. The ethyl groups decompose at higher temperatures and form ethylene via a β -hydride elimination reaction. Isotopic labeling experiments are used to confirm this reaction step. This is in contrast to the Si(100) surface where both α - and β -hydride elimination is observed for the decomposition of surface ethyl groups. Low energy electron diffraction is used to evaluate the quality of the deposited germanium films. © 1997 American Vacuum Society. [S0734-2101(97)58603-9]

I. INTRODUCTION

As the explosive development of the semiconductor industry continues, the size of microelectronic and optical devices is smaller and the structure of these devices is more complex. The atomic level understanding of these structures is crucial for continued development of methods for fabrication of these devices. With the maturing of ultrahigh vacuum (UHV) technology and sophisticated analytical tools, such as Auger electron spectroscopy (AES), low energy electron diffraction (LEED) and temperature programmed desorption (TPD), the atomic level investigation of these fabrication processes and the development of new synthetic methods are being performed by a number of research laboratories. Based on the results of this research, new technologies have been developed and novel structures have been synthesized, for example, VLSI structures, quantum well lasers, high electron mobility transistors, and superlattice avalanche photodiodes.¹ These device implementations give added impetus to research work.

Coincident with these developments, research related to epitaxial growth of semiconductor films from atomic and molecular beams and chemical vapors has also grown rapidly. The main types of processes studied include molecular beam epitaxy (MBE), chemical vapor deposition (CVD) and atomic layer epitaxy (ALE). In CVD, chemical components in the vapor phase react to form a thin film at a substrate surface. The growth is at conditions near thermodynamic equilibrium and is mostly controlled by diffusional processes occurring in the crystallizing phase surrounding the substrate crystal. The unique attributes of CVD are conformal film growth and selective area growth.

ALE is a further refinement in the evolution of CVD growth techniques, that can control film thickness to one monolayer.²⁻⁴ ALE is based on chemical reactions at the surface of a substrate; it is surface-controlled growth. The reactants are delivered as pulses of neutral molecules or at-

oms in alternating fashion, either as chopped beams in high vacuum or as switched streams of vapor. The substrate temperature and gas pressure or flux are selected to allow one molecular layer of the precursor to chemisorb and react. The film grows stepwise. The thermal decomposition of mono-, di-, and triethylgermane on silicon was studied to examine the possible use of these molecules as CVD and ALE precursors.⁵⁻¹³ Each of these molecules was able to deposit Ge in an ALE reaction cycle. H₂ and C₂H₄ were observed as the gas phase products of the surface reaction.

A similar study examining the surface chemistry of GeH₂Et₂ on Ge(100) was recently reported.¹⁴ Again surface ethyl groups were detected. These ethyl groups decomposed to form ethylene. However little insight as to the formation of ethylene was given. The pathway(s) for ethylene desorption from the decomposition of surface ethyl groups on Si(100) and Si(111) were examined.^{15,16} There are two possible pathways. One reaction sequence is α -hydride elimination followed by a hydrogen shift in order to generate ethylene. The other sequence is a β -hydride elimination. β -hydride elimination is mostly proposed for the removal of surface ethyl groups.^{5,6,8,9,12,14,16,17} An *ab initio* calculation for the gas phase monoethylsilane shows that β -hydride elimination is the lowest energy pathway to yield ethylene.¹⁸ One approach to examine these pathways used deuterium labeling of the hydrogen within the ethyl group to distinguish between the two mechanisms on silicon surfaces.¹⁵ The results showed that both α -hydride and β -hydride elimination are involved in producing ethylene. The branching ratio of the two mechanisms (β/α) showed an isotope effect and β -hydride elimination was the dominant pathway for ethyl decomposition on Si when exposed to EtBr-*d*₃.

In this article we report the reactions of diethylgermane (GeH₂Et₂), triethylgermane (GeHET₃), and ethylbromide (EtBr) on the Ge(100) surface. These studies provide a direct comparison to those previously completed on silicon surfaces. Room temperature exposure of GeH₂Et₂, GeHET₃, or EtBr to Ge(100) results in dissociative adsorption of each molecule and the formation of surface ethyl groups. These ethyl groups decompose at higher temperatures to form

^{a)}Present address: Dept. of Electrical and Computer Engineering, University of Cincinnati, Cincinnati, OH 45221-0030.

^{b)}Author to whom all correspondence should be addressed; Electronic mail: chemcmg@showme.missouri.edu

ethylene. Deuterium labeling of the ethyl groups allows for the determination of the decomposition pathways to ethylene.

II. EXPERIMENT

The experiments are performed in a custom-built stainless steel UHV chamber and the chamber is pumped by a 500 ℓ/s turbomolecular pump (Balzers TPU 520). The main chamber is equipped with a quadrupole mass analyzer (UTI model 100C) for residual gas analysis and TPD studies, a set of reverse-view LEED optics (Princeton Research Instruments), and an ion gun for sputtering. The base pressure of the system is 1.5×10^{-10} Torr with a typical working pressure of 2.0×10^{-10} Torr.

The samples are cleaved into $10 \times 25 \times 0.2$ mm rectangles from *n*-type Ge(100) substrates [Eagle-Picher, $\pm 0.5^\circ$ of the (100) plane, Sb doped, 0.04–0.4 Ω cm resistivity]. Before placing the sample into the chamber, the Ge(100) substrate is degreased by (a) ultrasonically rinsing in trichloroethylene, acetone, and methanol for 3 min each, (b) immediately blowing dry with dry nitrogen, and (c) ultrasonically rinsing in deionized water for 15 min to lower the contact resistance.¹⁹ The sample is held by molybdenum clamps for resistive heating and mounted to a manipulator. The sample temperature is monitored by a pair of Chromel–Alumel thermocouples attached to the back of the sample with Aremco 516 ceramic adhesive. Low energy electron diffraction is used to check the cleanliness and periodic order of the Ge(100) 2×1 surface. A clean surface is generated by the removal of the native oxide by repeated heating to 850 K in vacuum followed by ion sputtering (3 keV Ar^+ , 1 μA), and annealing at 850 K. The number of defects induced by sputtering, as observed by the sharpness of the LEED pattern, can be reduced by exposing the Ge sample to an apparent pressure of 5×10^{-8} Torr Ge_2H_6 (Voltaix, ultrahigh purity grade, minimum purity 99.999%) while the surface temperature is maintained at 570 K for about 5 min. The Ge_2H_6 gas flow is then turned off and the sample is annealed at 850 K before cooling. After several cycles of Ar^+ sputtering, annealing, Ge_2H_6 exposure, and annealing, a sharp 2×1 LEED pattern was observed for the Ge(100) surface.

1,1-bromoethane-*d*₂ (C/D/N Isotopes, Inc., 98.7 at. % D), 2,2,2-bromoethane-*d*₃ (C/D/N Isotopes, Inc., 99.2 at. % D), diethylgermane (Gelest, purity >98%), and triethylgermane (Gelest, purity >98%) are further purified by several freeze-pump-thaw degassing cycles and the purity of the gases is checked *in situ* by mass spectrometry. The exposures are reported as langmuirs (L) (1 L = 10^{-6} Torr sec) as measured directly by the ion gauge.

Temperature programmed experiments are conducted with a linear temperature ramp of 5 K s^{-1} with the crystal in line-of-sight of the quadrupole mass spectrometer. The coverage at saturation for hydrogen on Ge(100) at room temperature has been determined as 1 monolayer (ML) (1 ML = one adsorbate per surface Ge atom).^{14,20–23} The temperature programmed desorption area from a saturation coverage

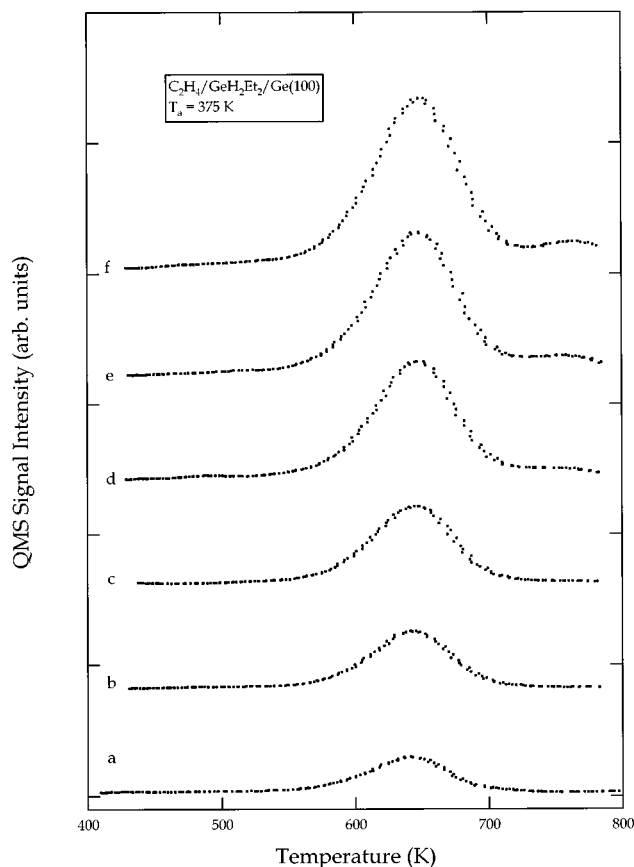


Fig. 1. TPD spectra of C_2H_4 following different exposures of GeH_2Et_2 at a surface temperature of 375 K. The exposures shown are (a) 0.09, (b) 0.9, (c) 9, (d) 90, (e) 300, and (f) 600 L.

of H atoms is then used as an internal standard for H_2 thermal desorption.

Some of the experiments reported here were repeated in a second UHV chamber that was previously described in detail.²⁴ This second chamber is equipped for TPD and AES studies. AES analysis of samples treated in the same fashion as described above revealed no carbon contamination after cleaning of the sample nor after the temperature ramp in TPD experiments using the molecules in this study.

III. RESULTS AND DISCUSSION

A. Diethylgermane and triethylgermane on Ge(100)

The adsorption and decomposition of GeH_2Et_2 and GeHEt_3 were followed by TPD. TPD spectra were obtained following different exposures of GeH_2Et_2 and GeHEt_3 to the Ge(100) at a surface temperature of 375 K. In the TPD studies, no parent fragment ions were detected. The only desorption products observed by TPD, after a search for other hydrocarbons such as C_2H_2 or C_2H_6 , were H_2 and C_2H_4 .

Figure 1 summarizes the C_2H_4 desorption resulting from the decomposition of GeH_2Et_2 . The C_2H_4 desorption spectra show a single desorption peak centered at 650 K. The intensity of the desorption state increases with increasing GeH_2Et_2 exposure. The ethylene desorption peak area satu-

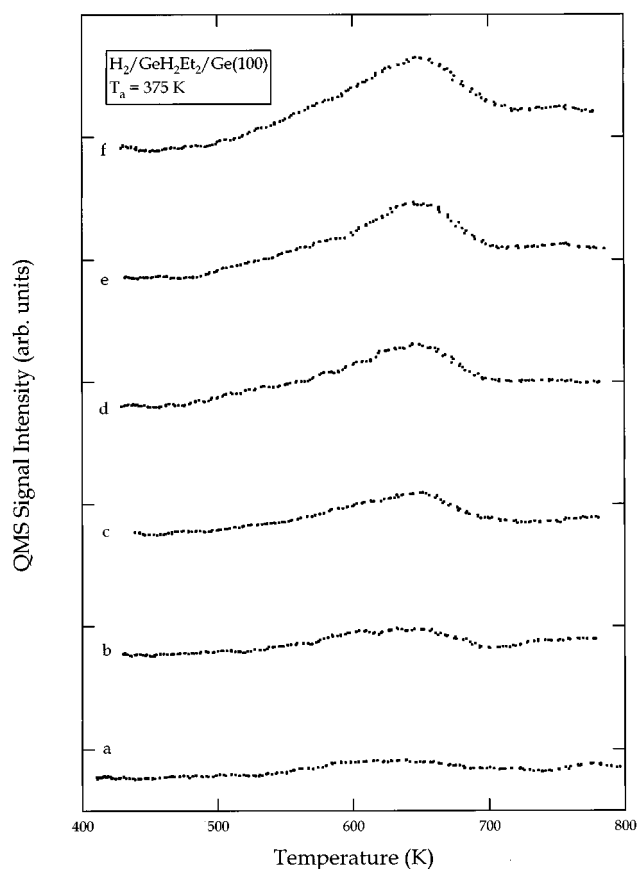


Fig. 2. TPD spectra of H_2 following different exposures of GeH_2Et_2 at a surface temperature of 375 K. The exposures shown are (a) 0.09, (b) 0.9, (c) 9, (d) 90, (e) 300, and (f) 600 L.

rates and remains constant for exposures greater than 600 L. The ethylene desorption kinetics were also determined. The entire data set can best be described as a first order desorption process with an activation energy for desorption of $45 \pm 1 \text{ kcal mol}^{-1}$ and a preexponential factor of $1 \times 10^{14 \pm 1} \text{ s}^{-1}$.

Figure 2 shows H_2 TPD spectra obtained following various exposures of GeH_2Et_2 to the $\text{Ge}(100)$ at a surface temperature of 375 K. The H_2 desorption peaks are broad compared to those obtained from atomic H (Ref. 25) or digermane exposures.²⁶ At the highest exposures [Fig. 2(f)], the main part of the desorption is centered at 650 K, the same temperature as the ethylene desorption. There is also a shoulder to the low temperature side of the main peak and the H_2 desorption that starts near 500 K. Since the desorption of H_2 from a clean Ge surface is at 575 K,^{21,22} the production of H_2 desorbing at 650 K is reaction limited. This broad H_2 desorption peak may be composed of two peaks: one consisting of H_2 from bare Ge sites and one of H_2 desorbing with the ethylene. The approximate position of the two peaks was determined by fitting the desorption spectra with two Gaussian functions. A typical fit of the desorption spectra yields two desorption states with peak maxima at 570 K and 645 K. The peak at 570 K is then most likely formed by recombinative hydrogen desorption from the germanium

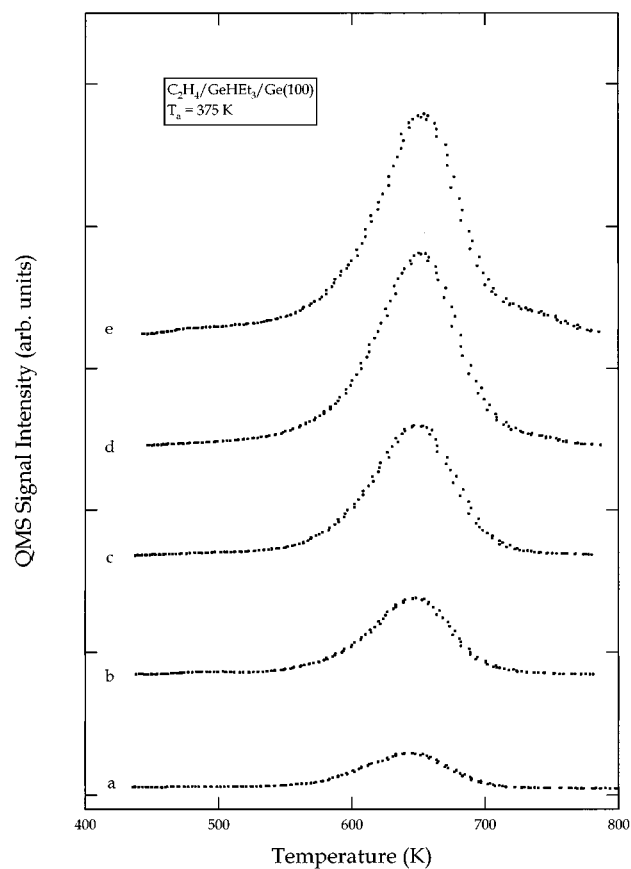


Fig. 3. TPD spectra of C_2H_4 following different exposures of GeHEt_3 at a surface temperature of 375 K. The exposures shown are (a) 0.09, (b) 0.9, (c) 9, (d) 90, and (e) 300 L.

monohydride phase. The peak at 645 K is formed by immediate recombinative desorption of hydrogen atoms that are generated by surface ethyl group decomposition which occurs at the same temperature (discussed further below).

Figure 3 shows the C_2H_4 desorption resulting from the decomposition of GeHEt_3 . The overall desorption features (peak temperatures and desorption rates) are similar to those obtained for GeH_2Et_2 . The main difference is that the desorption peak areas are larger for a given exposure. This difference can be related simply to the number of ethyl groups contained in each starting molecule.

The H_2 desorption spectra from the decomposition of GeHEt_3 are summarized in Figure 4. Again the H_2 desorption spectra are similar to those obtained for GeH_2Et_2 . The desorption peak is broad and asymmetric to the low temperature side. However, the majority of the H_2 desorption occurs near 650 K. A deconvolution of Fig. 4(e), using two Gaussian peaks, yields peak temperatures at 655 K and 590 K.

In these thermal desorption studies of GeH_2Et_2 and GeHEt_3 on $\text{Ge}(100)$, no parent fragments are detected in the TPD spectra obtained following different exposures to $\text{Ge}(100)$. No carbon was detected on the Ge surface after the TPD studies within the detection limit of AES. These two results indicate that the incident precursor molecules dissociatively chemisorbed on the surface, which is consistent

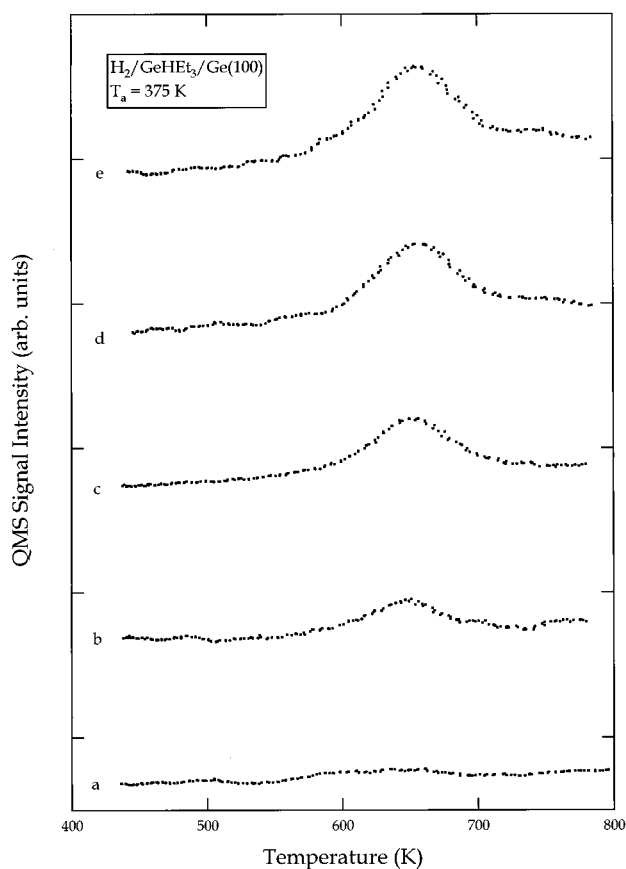


Fig. 4. TPD spectra of H_2 following different exposures of GeHEt_3 at a surface temperature of 375 K. The exposures shown are (a) 0.09, (b) 0.9, (c) 9, (d) 90, and (e) 300 L.

with the dissociative adsorption of GeH_2Et_2 on $\text{Ge}(100)$ observed previously by high resolution electron energy loss spectroscopy (HREELS).¹⁴ The TPD peak observed at 570 K is due to the recombinative desorption of H atoms and the second peak at 650 K is due to the desorption of H atoms generated by hydride elimination of surface ethyl groups. If the two H atoms attached to Ge in GeH_2Et_2 are transferred to $\text{Ge}(100)$ upon adsorption, two peaks should be observed in TPD for H_2 with the same area because the hydride elimination of the two ethyl groups will generate two H atoms. In the H_2 TPD results, there is only one peak at 650 K with a low temperature shoulder. This peak was fit by two Gaussian peaks at 570 and 645 K. The area for the peak at 570 K is only 26% of the peak at 645 K. In the GeHEt_3 TPD experiments, the low temperature shoulder in the H_2 desorption peak at 650 K is smaller than that observed for GeH_2Et_2 . Fitting the H_2 desorption spectrum in this case revealed that the peak area at 590 K is 9% of that at 655 K. These results suggest that GeH_2Et_2 and GeHEt_3 dissociatively adsorb as more than one organometallic species, such as $\text{GeH}(\text{C}_2\text{H}_5)_x$ ($x=0-3$). If GeH_2Et_2 and GeHEt_3 transfer small amounts of H to the surface upon adsorption to the $\text{Ge}(100)$ surface, and the adsorbed organometallic species decompose at 650 K, the above H_2 TPD spectra could be obtained.

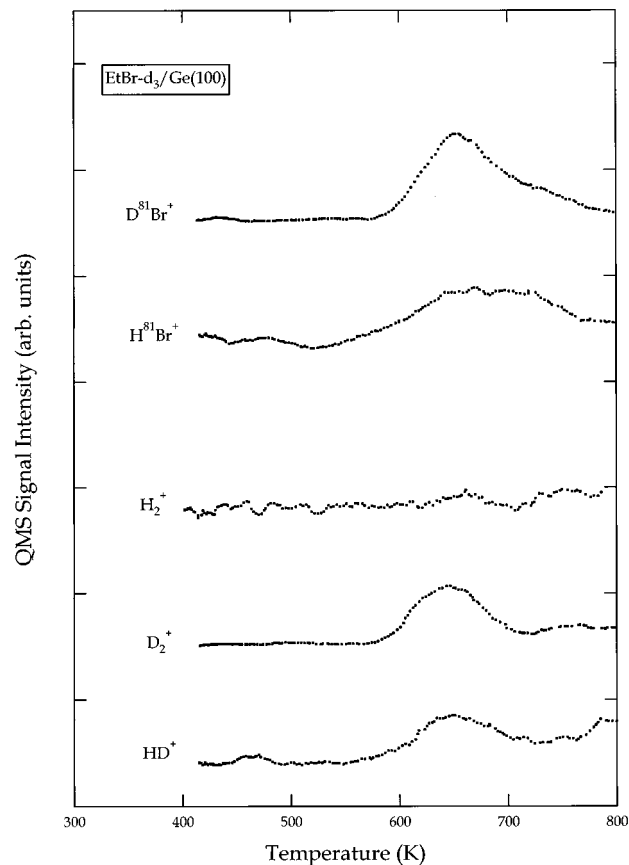


Fig. 5. TPD spectra following a 300 L exposure of EtBr-d_3 to $\text{Ge}(100)$ at a surface temperature of 375 K.

B. Ethyl group decomposition on $\text{Ge}(100)$

The decomposition of $\text{CH}_3\text{CD}_2(\text{EtBr-d}_2)$ and $\text{CD}_3\text{CH}_2(\text{EtBr-d}_3)$ on the $\text{Ge}(100)$ surface were followed by TPD to gain further insight about ethyl group decomposition on Ge. No TPD signal was detected for either parent EtBr molecule.

The exposure of EtBr-d_3 or EtBr-d_2 to the Ge surface, followed by TPD analysis, yielded ethylene as the major desorption product. The ethylene desorption spectra were identical to those obtained using GeH_2Et_2 or GeHEt_3 and are therefore not reproduced. The ethylene desorption is centered at 650 K and the peak does not shift in temperature with the increasing of EtBr-d_3 or EtBr-d_2 exposures. These results indicate that (1) EtBr-d_3 and EtBr-d_2 probably dissociate to CH_2CD_3 or CD_2CH_3 and Br upon adsorption onto $\text{Ge}(100)$. Similar behavior is observed for EtBr-d_3 and EtBr-d_2 adsorption on $\text{Si}(100)$.^{15,16} The ethylene is then produced from the decomposition of surface ethyl groups. (2) The desorption of ethylene is a local effect and not affected by the coadsorbed atoms, such as Ge and Br.

Figure 5 shows the TPD spectra for a series of species that desorb from Ge as a result of EtBr-d_3 decomposition. TPD spectra of D^{81}Br^+ , H^{81}Br^+ , H_2^+ , D_2^+ , and HD^+ following a 300 L exposure of EtBr-d_3 to $\text{Ge}(100)$ at a sample temperature of 375 K are shown. The H_2 TPD spectrum is featureless. D_2 and HD desorb at 650 K, the same temperature as

the ethylene desorption. HBr and DBr desorb at 660 K and the peak areas for HBr and DBr are about two times larger than those of D₂ and HD. Based on desorption peak areas, the formation of hydrogenbromide is the main pathway for desorption of hydrogen (H or D) and Br. The observation of D₂ and DBr indicates that β -hydride elimination played a role in the decomposition of the surface ethyl group since the D was attached to β -C of the ethyl group. The observation of HD and HBr indicates that the α -hydride elimination also played a role in the decomposition of the surface ethyl group since H was attached to α -C of the ethyl group. The branching ratio for the two mechanistic pathways can be estimated by the following equation:

$$\frac{\beta}{\alpha} = \frac{2\theta_{D_2} + \theta_{D^{79}Br} + \theta_{D^{81}Br} + \theta_{HD}}{2\theta_{H_2} + \theta_{HD} + \theta_{H^{79}Br} + \theta_{H^{81}Br}} \quad (1)$$

In equation (1), θ_x represents the TPD peak area for species x . The numerator is the total number of D atoms generated by β -hydride elimination and the denominator is the number of H atoms generated by α -hydride elimination. From TPD data (not shown), the TPD peak area of H⁷⁹Br is the same as that of H⁸¹Br within experimental error, which agrees with the natural isotopic abundance for bromine (50.69% for ⁷⁹Br and 49.31% for ⁸¹Br).²⁷ If the ratio of D⁷⁹Br and D⁸¹Br areas is also 1:1, then equation (1) can be rewritten as

$$\frac{\beta}{\alpha} = \frac{2\theta_{D_2} + 2\theta_{D^{81}Br} + \theta_{HD}}{2\theta_{H_2} + \theta_{HD} + 2\theta_{H^{81}Br}} \quad (2)$$

With equation (2), a value for $\beta/\alpha=1.41$ for a 9 L EtBr-*d*₃ exposure and $\beta/\alpha=1.76$ for a 300 L EtBr-*d*₃ exposure is obtained. The value of this ratio is greater than 1 for all measured exposures indicating that β -hydride elimination is favored over α -hydride elimination.

Figure 6 shows TPD spectra of D⁸¹Br, H⁸¹Br, H₂, D₂, and HD obtained following a 300 L EtBr-*d*₂ exposure to Ge(100) at a sample temperature of 373 K. The TPD spectrum for HBr shows a peak at 670 K and the H₂ spectrum shows only a small peak. In contrast to the experiments with EtBr-*d*₃ no D containing compounds other than C₂H₂D₂ are observed. This means that the H attached to β -C is transferred to the Ge surface and recombines with adsorbed Br atoms to desorb as HBr. These observations indicate that β -hydride elimination is the only pathway for ethylene formation on the Ge(100) surface.

The secondary reaction product (H or D) was followed and used to determine the branching ratio of the hydride elimination reaction because it is difficult to separate the different ethylene fragments when using electron impact ionization at an ionization energy of 70 eV. This is also why we are not able at this time to explore the kinetic isotope effects of this reaction in more detail.

From previous studies,^{22,28-30} there are two possible pathways for forming HBr. One pathway is recombination of surface H and surface Br atoms. A TPD study from D'Evelyn *et al.*²² showed that H₂ desorbed at 575 K for 0.1 ML and 565 K for 0.5 ML. HBr desorbed at 590 K for 0.1

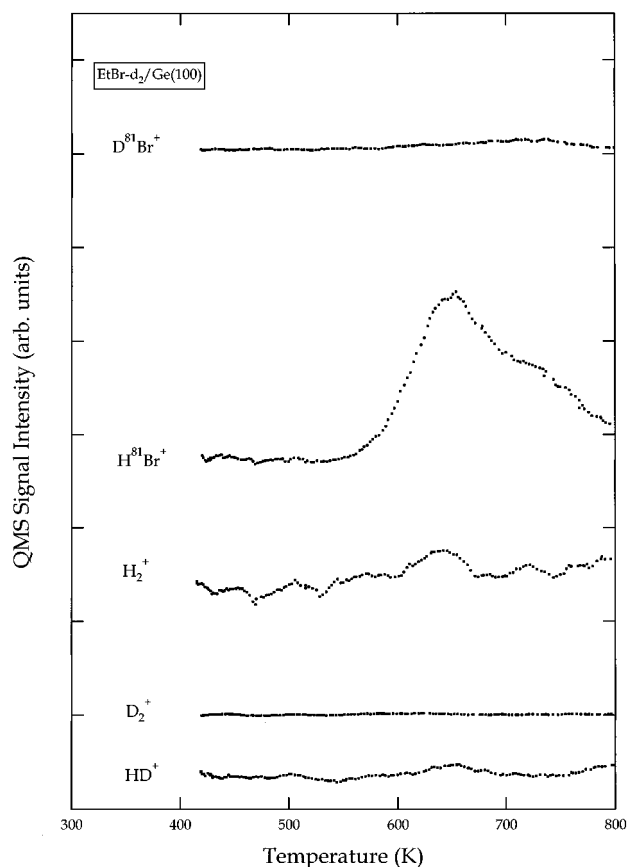


Fig. 6. TPD spectra following a 300 L exposure of EtBr-*d*₂ to Ge(100) at a surface temperature of 375 K.

ML and shifted to 582 K for 0.5 ML. HBr has near-first-order desorption kinetics. The other possible channel is H atom extraction of surface Br. Several studies²⁸⁻³⁰ indicate that H atom extraction of Br adsorbed on Si(100) has an activation energy of almost zero, the desorption is first order, and it is only dependent on the coverage of Br. In this work, the surface Br was generated by dissociative adsorption of EtBr-*d*₃ at 373 K, and the H atoms were generated by decomposition of ethyl groups at 650 K. So at this temperature, the H atoms may combine with surface Br by diffusion across the Ge surface or by directly combining with Br without transferring first to the surface.

The deuterated EtBr experiments show that there is an isotope effect in the thermal decomposition of ethyl group on the Ge(100) surface. β -hydride elimination is the exclusive mechanism for the removal of the surface α -deuterated ethyl group (CD₂CH₃). Both α - and β -hydride elimination are observed for the removal of the surface β -deuterated ethyl group (CH₂CD₃). The reason for α elimination is probably due to H-C _{α} having a larger vibrational energy compared to D-C _{β} , because the D atom is two times heavier than the H atom. The H-C _{α} bond can break and combine with surface Br or D by α -hydride elimination. Without this isotope effect, β -hydride elimination would be the only mechanism for the removal of ethyl groups on Ge(100).

IV. CONCLUSIONS

We have studied the surface chemistry of GeH₂Et₂ and GeHET₃ on the Ge(100) surface. The compounds dissociatively adsorb producing ethyl groups and adsorbed hydrogen. As the surface is heated, the hydrogen produced during the adsorption step desorbs at 570 K, the temperature for the desorption of hydrogen from a monohydride covered Ge(100) surface. The ethyl groups undergo β -hydride elimination at 650 K, leave the surface as ethylene, and deposit atomic hydrogen on the surface. The hydrogen immediately recombines to form molecular H₂ and desorbs producing simultaneous C₂H₄ and H₂ desorption peaks.

ACKNOWLEDGMENTS

The authors are happy to acknowledge the National Science Foundation (Grant No. CHE-9100429) and the University of Missouri Research Board for support of this research. One of the authors (C.M.G.) also acknowledges the National Science Foundation for a Young Investigator Award.

¹M. A. Herman and H. Sitter, *Molecular Beam Epitaxy* (Springer, Berlin, 1989).

²T. Suntola, *Thin Solid Films* **96**, 216 (1992).

³T. Suntola and M. Simpson, *Atomic Layer Epitaxy* (Chapman and Hall, New York, 1990).

⁴J. M. Heitzinger, J. M. White, and J. G. Ekerdt, *Surf. Sci.* **299/300**, 892 (1993).

⁵A. Mahajan, B. K. Kellerman, N. M. Russell, S. Banerjee, A. Campion, J. G. Ekerdt, A. Tasch, J. M. White, and D. J. Bonser, *J. Vac. Sci. Technol. A* **12**, 2265 (1994).

⁶P. A. Coon, M. L. Wise, A. C. Dillon, and S. M. George, *Mater. Res. Soc. Symp. Proc.* **282**, 413 (1993).

⁷A. C. Dillon, M. B. Robinson, and S. M. George, *Surf. Sci.* **286**, L535 (1993).

⁸P. A. Coon, M. L. Wise, and S. M. George, *J. Chem. Phys.* **98**, 7485 (1993).

⁹P. A. Coon, M. L. Wise, Z. H. Walker, S. M. George, and D. A. Roberts, *Appl. Phys. Lett.* **60**, 2002 (1992).

¹⁰C. M. Greenlief, D.-A. Klug, and L. A. Keeling, *Mater. Res. Soc. Symp. Proc.* **282**, 427 (1993).

¹¹Y. Takahashi, H. Ishii, and K. Fujinaga, *J. Electrochem. Soc.* **136**, 1826 (1989).

¹²W. Du, L. A. Keeling, and C. M. Greenlief, *J. Vac. Sci. Technol. A* **12**, 2281 (1994).

¹³L. A. Keeling, Ph.D. dissertation, University of Missouri, 1995.

¹⁴A. Mahajan, B. K. Kellerman, J. M. Heitzinger, S. Banerjee, A. Tasch, J. M. White, and J. G. Ekerdt, *J. Vac. Sci. Technol. A* **13**, 1461 (1995).

¹⁵D.-A. Klug and C. M. Greenlief, *J. Vac. Sci. Technol. A* **14**, 1826 (1996).

¹⁶L. A. Keeling, L. Chen, C. M. Greenlief, A. Mahajan, and D. Bonser, *Chem. Phys. Lett.* **217**, 136 (1994).

¹⁷P. A. Coon, M. L. Wise, A. C. Dillon, M. B. Robinson, and S. M. George, *J. Vac. Sci. Technol. B* **10**, 221 (1992).

¹⁸J. S. Francisco and H. B. Schlegel, *J. Chem. Phys.* **88**, 3736 (1988).

¹⁹X.-J. Zhang, G. Xue, A. Agarwal, R. Tsu, M.-A. Hasan, J. E. Greene, and A. Rockett, *J. Vac. Sci. Technol. A* **11**, 2553 (1993).

²⁰S. M. Cohen, Y. L. Yang, E. Rouchouze, T. Jin, and M. P. D'Evelyn, *J. Vac. Sci. Technol. A* **10**, 2166 (1992).

²¹M. P. D'Evelyn, S. M. Cohen, E. Rouchouze, and Y. L. Yang, *J. Chem. Phys.* **98**, 3560 (1993).

²²M. P. D'Evelyn, Y. L. Yang, and S. M. Cohen, *J. Chem. Phys.* **101**, 2463 (1994).

²³L. B. Lewis, J. Segall, and K. C. Janda, *J. Chem. Phys.* **102**, 7222 (1995).

²⁴C. M. Greenlief and D. A. Klug, *J. Phys. Chem.* **96**, 5424 (1992).

²⁵L. Surnev and M. Tikhov, *Surf. Sci.* **138**, 40 (1984).

²⁶J. Chen and C. M. Greenlief (unpublished).

²⁷*CRC Handbook of Chemistry and Physics*, edited by R. C. Weast (Chemical Rubber, Cleveland, 1975).

²⁸C. C. Cheng, S. R. Lucas, H. Gutleben, W. J. Choyke, and J. T. Yates, Jr., *J. Am. Chem. Soc.* **114**, 1249 (1992).

²⁹D. D. Koleske and S. M. Gates, *J. Chem. Phys.* **99**, 8218 (1993).

³⁰D. D. Koleske and S. M. Gates, *J. Chem. Phys.* **98**, 5091 (1993).